



Published in final edited form as:

Biochemistry. 2013 September 10; 52(36): . doi:10.1021/bi400613h.

Structural Consequences of Cysteinylation of Cu/Zn-Superoxide Dismutase

Jared R. Auclair^{1,2}, Heather R. Brodtkin^{1,3}, J. Alejandro D'Aquino¹, Gregory A. Petsko¹, Dagmar Ringe¹, and Jeffrey N. Agar^{1,2}

¹Departments of Biochemistry and Chemistry and Rosenstiel Basic Medical Sciences Research Center, Brandeis University, Waltham, MA, USA

Abstract

The metalloenzyme Cu/Zn-superoxide dismutase (SOD1) catalyzes the reduction of superoxide anions into molecular oxygen and hydrogen peroxide. Hydrogen peroxide can oxidize SOD1, resulting in aberrant protein conformational changes, disruption of SOD1 function, and DNA damage. Cells may have evolved mechanisms of regulation that prevent such oxidation. We observed that cysteinylation of Cysteine 111 (Cys₁₁₁) of SOD1 prevents oxidation by peroxide¹. In this article, we characterize cysteinylated SOD1 using differential scanning fluorimetry and X-ray crystallography. The stoichiometry of binding was one cysteine per SOD1 dimer, and there does not appear to be free volume for a second cysteine without disrupting the dimer interface. Much of the three dimensional structure of SOD1 is unaffected by cysteinylation. However, local conformational changes are observed in the cysteinylated monomer that include changes in conformation of the electrostatic loop (loop VII; residues 133-144) and the dimer interface (loop VI; residues 102-115). In addition, our data shows how cysteinylation precludes oxidation of Cysteine 111 and suggests possible cross-talk between the dimer interface and the electrostatic loop.

Introduction

Cu/Zn-superoxide dismutase (SOD1) is a 153 amino acid homodimer that catalyzes the metaldependent reduction of superoxide anions (O₂⁻) to hydrogen peroxide (H₂O₂) and oxygen (O₂)². One of the products of the reaction, hydrogen peroxide, can damage the enzyme: it oxidizes Cys₁₁₁ first, and then Trp32 and active site histides, leading to inactivation of SOD1^{3,4}. This activity-dependent inactivation leads to an increase in superoxide anions, which in turn, produces negative effects such as aberrant protein conformational changes, disruption of enzyme function, and mutation of DNA, etc.⁵⁻⁷. In a sister manuscript we demonstrate cysteinylation of Cys₁₁₁ and show that cysteinylation prevents oxidation of SOD1 in vitro¹. This post-translational modification raises the possibility that cysteinylation is part of a regulatory mechanism that protects SOD1 from oxidation by its product, hydrogen peroxide.

Cysteinylation is a post-translational modification that remains largely uncharacterized because protein preparations are generally treated with disulfide reducing agents such as

Corresponding Author: agar@brandeis.edu (781)-736-2425.

²Current Address: Department of Chemistry and Chemical Biology and Pharmaceutical Sciences and the Barnett Institute, Northeastern University, Boston, MA, USA

³Current Address: Alkermes, Waltham, MA, USA

Supporting Information: We have included a supplemental table and figure. This material is available free of charge via the Internet at <http://pubs.acs.org>

dithiothreitol (DTT), 2-mercaptoethanol (β -Me), or *tris*(2-carboxyethyl)phosphine (TCEP), which remove cysteinylation. Despite this, cysteinylation has been observed, but not well characterized, in transthyretin (TTR), human serum albumin, and the k1 light chain from an amyloid patient^{8,9}. Cysteinylation has also been observed during oxidative stress treatment of *Bacillus subtilis* strains, where it may protect cysteine residues from oxidation¹⁰.

To better understand SOD1 cysteinylation, we set out to characterize its structure using differential scanning fluorimetry and X-ray crystallography. We present the first structural analysis of cysteinylated SOD1, and to the best of our knowledge of any cysteinylated protein.

Methods

Protein Expression and Purification

The construct for expression of human SOD1 (hSOD1) in *S. cerevisiae* was obtained through the generous gift of Dr. P. John Hart, Ph.D. (University of Texas Health Science Center, San Antonio). Expression and purification was carried out as previously published^{11,12}. Briefly, hSOD1 in the yeast expression vector YEp-351 was transformed into EGY118 Δ SOD1 yeast and grown at 30 °C for approximately 48 hours. Cultures were pelleted, lysed using 0.5 mm glass beads and a blender, and subjected to a 60 % ammonium sulfate cut. After ammonium sulfate precipitation, the sample was pelleted and the supernatant was diluted with 0.19 volumes of a low salt buffer (50 mM sodium phosphate, 150 mM sodium chloride, 0.1 M EDTA, 0.25 mM DTT, pH 7.0) to a final concentration of 2.0 M ammonium sulfate. This sample was then purified using a phenyl-sepharose 6 fast flow (high sub) hydrophobic interaction chromatography column (GE Life Sciences) using a 300 mL linearly decreasing salt gradient from a high salt buffer (2.0 M ammonium sulfate, 50 mM sodium phosphate, 150 mM sodium chloride, 0.1 M EDTA, 0.25 mM DTT, pH 7.0) to a low salt buffer (50 mM sodium phosphate, 150 mM sodium chloride, 0.1 M EDTA, 0.25 mM DTT, pH 7.0). Samples containing SOD1 were eluted between 1.6-1.1 M ammonium sulfate, pooled and exchanged to a 10 mM Tris, pH 8.0 buffer. The protein was then loaded onto a Mono Q 10/100 anion exchange chromatography column (GE Life Sciences) and eluted using a 200 mL linearly increasing salt gradient from a low salt buffer (10 mM Tris, pH 8.0) to a high salt buffer (10 mM Tris, pH 8.0, 1 M sodium chloride). The gradient was run from 0-30 % 10 mM Tris, pH 8.0, 1 M sodium chloride and SOD1 eluted between 5-12 % 10 mM Tris, pH 8.0, 1 M sodium chloride. SOD1 protein was diluted into 50 % acetonitrile, 0.1 % formic acid (MALDI) or 5 % acetonitrile, 0.1 % formic acid (FTMS); confirmed via MALDI-TOF and FTMS analysis; and quantified using the Bradford assay with yields of 6 mg/8L (0.75 mg/L). In addition, the majority of SOD1 samples are fully metallated as determined by intact mass analysis using a fourier transform mass spectrometer, which is in agreement with previous ICP-MS analysis we performed on a representative sample¹³.

Crystallization, Data Collection and Refinement

Crystals of cysteinylated SOD1 were grown using the hanging drop method at 25 °C. SOD1 was cysteinylated by incubating an 8 mg/mL stock solution of protein with 40-fold molar excess of cysteine (20.7 mM) for 30-60 minutes prior to setting the drop. Four microliter drops were formed by mixing equal volumes of cysteinylated protein and a crystallization solution containing 0.1 M MES, pH 6.25, 20% PEG 3350. After 1-3 weeks, crystals suitable for X-ray crystallography appeared in the drops. The crystals were harvested directly from the drops, transferred to a solution containing 20% glycerol in 0.1 M MES, pH 6.25, 20% PEG 3350 as a cryoprotectant, and subsequently flash frozen in liquid nitrogen prior to data collection.

Data were collected at beamline 23-ID-B at GM/CA-CAT (Advanced Photon Source (APS), Argonne National Laboratory (ANL), Argonne, IL) at 100 K using a MarMosaic CCD detector. Diffraction images were integrated and scaled using HKL2000¹⁴. The integrated and scaled file from HKL2000 was used to assess the quality of the data and to rule out the possibility of twinning. We also exploited the graphics provided by the twinning server¹⁵ to visualize how our data compared to twinned data (Supplemental Figure S1). The crystals have the symmetry of space group $P6_3$ with unit cell dimensions $a = b = 113.1 \text{ \AA}$, $c = 70.6 \text{ \AA}$, $\alpha = \beta = 90^\circ$ and $\gamma = 120^\circ$.

The structure was solved by molecular replacement using PHENIX AutoMR¹⁶ and the coordinates of wild-type human SOD1 (PDB entry 1SPD¹⁷) were used as a starting model. The diffraction anisotropy server at the Molecular Biology Institute at UCLA (<http://services.mbi.ucla.edu/anisotropy>) was used to correct for anisotropy¹⁸.

In order to model the cysteine modification, a PDB file with cysteine only was created, opened in Coot and then modeled into the appropriate density and merged with the existing PDB. After a round of simulated annealing, multiple cycles of iterative manual building were performed in Coot¹⁹ and refined against an amplitude-based maximum-likelihood target function in PHENIX until the R_{free} could no longer be reduced. In addition, anisotropic refinements (18 TLS groups selected by PHENIX), water picking with PHENIX, and group B-factors were used in refinement. The atomic coordinates of cysteinylated SOD1 have been deposited in the Protein Data Bank (PDB 4FF9).

Differential Scanning Fluorimetry (DSF)

The melting temperature of SOD1 was monitored using differential scanning fluorimetry in the presence or absence of cysteine and hydrogen peroxide. In the first sequence of reactions, 20 μM SOD1 was incubated with 40-fold molar excess of cysteine (800 μM), 20 \times SYPROTM Orange, and added to a 96-well plate. In the second sequence of reactions, 20 μM SOD1 was incubated with 500-fold molar excess of hydrogen peroxide (10 mM), 20 \times SYPROTM Orange, and added to a 96-well plate. Reactions were diluted 1:1 (10 μM SOD1 final concentration) prior to analysis. The melting temperature of the protein was monitored using an RT-PCR machine (Applied Biosystems) with a 0.3 $^\circ\text{C}$ increase in temperature every minute from 25-100 $^\circ\text{C}$. Data were analyzed by subtracting a blank without protein from each respective well, normalized to 1, and temperature versus relative fluorescence was plotted²⁰. Reactions were repeated in triplicate.

Results

SOD1 is monocysteinylated

Following in vitro cysteinylated, mass spectrometry studies showed a mixture of unmodified and cysteinylated SOD1 monomer. Because the mass spectrometry methods dissociate the labile SOD1 dimer before detection, they could not, however, conclusively differentiate between there being monocysteinylated SOD1 dimer, or a mixture of dicysteinylated SOD1 dimer (each Cys111 residue modified) and unmodified dimer. The X-ray crystal structure of SOD1-cys was consistent with a binding stoichiometry of one cysteine attached to a single Cys₁₁₁ of the SOD1 dimer (Figure 1). There does not appear to be free volume for a second cysteine to modify the two-fold related Cys₁₁₁ on the opposite subunit without disrupting the dimer interface.

Cysteinylation of Cys₁₁₁ perturbs the local structure of the dimer interface (loop VI) and the electrostatic loop (loop VII)

We solved the crystal structure of SOD1-cys to 2.5 Å resolution, after screening over 40 different crystals using different crystallization and cryo-preservation conditions (Supplemental Table 1). Only one condition revealed cysteinylation on one monomer. The global structure of cysteinylated SOD1 was similar to that of other structures for this enzyme deposited in the PDB (Figure 1A). Superimposing the coordinates of wild type SOD1 (PDB ID: 1SPD) and SOD1-cys (this work) yields an RMSD of 1.0 Å over 153 α atoms for the α chain and 1.0 Å for 151 α atoms for the β chain. The refined model contains one homodimer in the asymmetric unit, 2 copper ions and 2 zinc ions (fully occupied), one cysteine modification on the β chain, and 24 waters. Details of the structure determination and refinement parameters are listed in Table 1. In addition, the protein exhibits good geometry where 88.7 % of the residues are in the most favored region of the Ramachandran analysis, with 8.9 % in the allowed regions, and 2.4 % outliers (7 total). Of those outliers, two were at the N-terminus, two were at the dimer interface, and two were in loops. There was missing density for the side chains of residues 3, 23, 24, and 36 on the α chain and 30, 36, 70, 100, 112 on the β chain, so those residues were modeled as alanine. In addition, no electron density was observed for residues 24 and 25 in loop II of the β chain, thus they were deleted from the model and not included in the final structure.

Superimposing wild type SOD (PDB ID: 1SPD¹⁷) and SOD-cys show some differences in two loop regions (loop VI, Figure 2 A, B and loop VII, Figure 2 C, D) of SOD1. Interestingly, the unmodified monomer (chain α) has similar structure at the dimer interface (particularly loop VI containing Cys₁₁₁) compared to the starting model (PDB ID: 1SPD), however the modified (cysteinylated) monomer (chain β) shows local perturbations of the dimer interface. This is evidenced by a 3.6 Å shift in loop VI between the Cα of Gly₁₀₈ in SOD-cys compared to the model structure (PDB ID: 1SPD) (Figure 2A compared to Figure 2B). In addition to the dimer interface, the cysteinylated monomer (chain β) also appears to have a local conformational change at the electrostatic loop (loop VII) as evidenced by a 3.4 Å shift between the Cα of Gly₁₃₀ in SOD-cys compared to the model structure (Figure 2C compared to Figure 2D).

Oxidation destabilized SOD1

Differential scanning fluorimetry (DSF) was used to measure the thermal stability of SOD1, oxidized SOD1 (SOD1-ox), and SOD1-cys. Fluorescence signal was monitored as native, oxidized, and cysteinylated SOD1 samples were heated in the presence of a fluorescent dye, respectively. Oxidation decreased the melting temperature (T_m) of SOD1 approximately 23 °C whereas cysteinylation decreased the melting temperature approximately 5 °C (Figure 3), thus suggesting oxidation had a profound effect on SOD1 stability compared to unmodified and cysteinylated SOD1.

Discussion

Here we present a structural analysis of SOD1 modified by cysteine (cysteinylated). The crystal structure suggests that the global structure of SOD1 is conserved upon modification. The 2.5 Å SOD1-cys crystal structure suggests that Cys₁₁₁ is the site of modification and that only one cysteine modification per dimer occurs, due to steric restriction of the symmetry-related site when the first one is modified. Local conformational changes were observed at the site of the modification in the dimer interface (loop VI) and at the distal electrostatic loop (loop VII) of the modified monomer (chain β); these conformational changes were not observed in the unmodified monomer (chain α), and are thus, not likely due to crystal packing. In addition, these conformation changes are consistent with allosteric

cross-talk between loop VI and loop VII. Modification of the electrostatic loop is interesting considering that was the one common effect of 13 ALS-causing mutations and the site for the gain-of-interaction found in Elam-Hart's crystal structures of fALS SOD1 variants^{21, 22}.

Because of an R-value of 27.6% and an R_{free} of 33.5%, we used phenix.xtriage to assess the quality of the data and to rule out the possibility of twinning. We also exploited the graphics provided by the twinning server¹⁵ to visualize how our data compared to twinned data (Supplemental Figure S1). The results of both twinning analyses showed that our data set was untwinned. After further inspection of the data, it became evident that the raw data show severe anisotropy and required a correction. Since the anisotropy lowers the resolution in one dimension of the frame, we expected our R-values to be somewhat higher as a result. We believe that an R-value of (27.6%) and R-free (33.5%) values are consistent with the anisotropic nature of the data set. Furthermore, the difference between R-value and R-free do not show evidence of over refinement. Finally, the crystal represents a mixture of modified and unmodified enzyme; in view of the conformational changes throughout the molecule produced by the modification (and only observed in the modified chain) that would mean any single mode cannot adequately account for all the scattering.

SOD1, SOD1-ox, and SOD1-cys stability was monitored using DSF and showed a 23 °C decrease in SOD1 melting temperature upon oxidation and only a 5 °C decrease in melting temperature upon cysteinylolation. This suggests oxidation causes a profound destabilization of SOD1 compared to unmodified and cysteinylated SOD1. Therefore, cysteinylolation only causes a small destabilization and, as we have shown previously can potentially abrogate the large destabilization due to oxidation¹. The small conformational changes in the electrostatic loop and dimer interface may be linked to SOD1-cys stability.

Interestingly, 2-mercaptoethanol-modified (2-ME) SOD1 has been described previously and its crystal structure has been solved^{23, 24} (PDB ID: 3T5W²⁴). The smaller 2-ME was able to modify both Cys₁₁₁ residues of the SOD1 dimer, change the electrostatic loop, and stabilize SOD1²³.

This is in comparison to monocysteinylolation, which changed the electrostatic loop but resulted in a small destabilization. Thus 2-ME SOD1 and monocysteinylated SOD1 share a similar structure, including the electrostatic loop, with the exception of changes observed in the residues immediately preceding cysteinylated Cys₁₁₁ (residues 108-111)²⁴. These data suggest that loop VI, in particular residues 108-111, and the electrostatic loop, may play a role in SOD1 stability.

SOD1 can be oxidized by one of its reaction products, hydrogen peroxide, which can cause protein conformational change and enzyme inactivation⁵⁻⁷, and promote proteolytic degradation^{25, 26}. Thus, it is possible that some sort of regulation (or protection) is present in the cell. We have previously observed cysteinylolation of SOD1 in nervous tissue, and that cysteinylolation protects against oxidation in vitro, suggesting cysteinylolation could play a protective role for SOD1 under conditions of oxidative stress. The data presented here suggest a structural mechanism where cysteinylolation can prevent oxidation of the modified cysteine in the dimer interface, whilst oxidation of the unmodified cysteine in the dimer interface can still occur. However, oxidation of just one cysteine at the dimer interface would not cause the electrostatic repulsion, and consequent dimer disruption, that would occur if both symmetry-related Cys₁₁₁ residues, which are only 7 Å apart, acquired permanent negative charges via oxidation.

Posttranslational modifications of SOD1, including oxidation of Cys₁₁₁, have been implicated in ALS, Parkinson's, and Alzheimer's diseases²⁷⁻³². Having a mechanism to block oxidation of Cys₁₁₁ could be advantageous in this sense as well. Further, both the

electrostatic loop³³ and dimer dissociation^{11, 29, 34, 35} have been implicated in fALS, and our SOD-cys structure suggests that cysteinylolation perturbs both of these regions. These local perturbations of SOD1 may prove to be crucial to the protein function and stability and provide a regulatory function in fALS.

Here, we present the structure of cysteinylated SOD1, and show that the modification may prevent the negative effects of oxidation on SOD1 and thereby function in a regulatory manner. In so doing, it may also prevent the deleterious effects oxidation may have on dimer stability, effects that have been postulated to lead to the SOD1-dependent form of ALS. Therapeutic strategies to mimic the effects of cysteinylolation may represent a new approach to the prevention of this disease.

Supplementary Material

Refer to Web version on PubMed Central for supplementary material.

Acknowledgments

Use of the Advanced Photon Source, an Office of Science User Facility operated for the U.S. Department of Energy (DOE) Office of Science by Argonne National Laboratory, was supported by the U.S. DOE under Contract No. DE-AC02-06CH11357. We thank Dr. P. John Hart for the generous gift of the YEP351-SOD1 plasmid and EGy118-(Δ SOD1) yeast cells used to express SOD1 in this study. We also thank members of the Agar and Petsko/Ringe Labs for thoughtful discussions, insights, and critically reviewing this manuscript.

This work was supported in part by a National Institutes of Health R21 (to J.N.A.) (1R21NS071256) and Fidelity Biosciences Research Initiative (to G.A.P. and D.R.)

References

1. Auclair JR, Johnson JJ, Liu Q, Salisbury JP, Rotunno M, Petsko GA, Ringe D, Brown RH Jr, Bosco DA, Agar J. Post-Translational Modification by Cysteine Protects Cu/Zn-Superoxide Dismutase from Oxidative Damage. 2013
2. McCord JM, Fridovich I. The reduction of cytochrome c by milk xanthine oxidase. *The Journal of biological chemistry*. 1968; 243:5753–5760. [PubMed: 4972775]
3. Karunakaran C, Zhang H, Crow JP, Antholine WE, Kalyanaraman B. Direct Probing of Copper Active Site and Free Radical Formed during Bicarbonate-dependent Peroxidase Activity of Bovine and Human Copper, Zinc-superoxide Dismutases: LOW-TEMPERATURE ELECTRON PARAMAGNETIC RESONANCE AND ELECTRON NUCLEAR DOUBLE RESONANCE STUDIES. *Journal of Biological Chemistry*. 2004; 279:32534–32540. [PubMed: 15123612]
4. Zhang H, Andrekopoulos C, Joseph J, Chandran K, Karoui H, Crow JP, Kalyanaraman B. Bicarbonate-dependent peroxidase activity of human Cu,Zn-superoxide dismutase induces covalent aggregation of protein: intermediacy of tryptophan-derived oxidation products. *J Biol Chem*. 2003; 278:24078–24089. [PubMed: 12686560]
5. Keithley EM, Canto C, Zheng QY, Wang X, Fischel-Ghodsian N, Johnson KR. Cu/Zn superoxide dismutase and age-related hearing loss. *Hear Res*. 2005; 209:76–85. [PubMed: 16055286]
6. Phillips JP, Tainer JA, Getzoff ED, Boulianne GL, Kirby K, Hilliker AJ. Subunit-destabilizing mutations in *Drosophila* copper/zinc superoxide dismutase: neuropathology and a model of dimer dysequilibrium. *P Natl Acad Sci USA*. 1995; 92:8574–8578.
7. Woodruff RC, Phillips JP, Hilliker AJ. Increased spontaneous DNA damage in Cu/Zn superoxide dismutase (SOD1) deficient *Drosophila*. *Genome*. 2004; 47:1029–1035. [PubMed: 15644960]
8. Kleinova M, Belgacem O, Pock K, Rizzi A, Buchacher A, Allmaier G. Characterization of cysteinylolation of pharmaceutical-grade human serum albumin by electrospray ionization mass spectrometry and low-energy collision-induced dissociation tandem mass spectrometry. *Rapid communications in mass spectrometry : RCM*. 2005; 19:2965–2973. [PubMed: 16178042]
9. Lim A, Wally J, Walsh MT, Skinner M, Costello CE. Identification and location of a cysteinyl posttranslational modification in an amyloidogenic kappa1 light chain protein by electrospray

- ionization and matrix-assisted laser desorption/ionization mass spectrometry. *Anal Biochem.* 2001; 295:45–56. [PubMed: 11476544]
10. Hochgrafe F, Mostertz J, Pother DC, Becher D, Helmann JD, Hecker M. S-cysteinylation is a general mechanism for thiol protection of *Bacillus subtilis* proteins after oxidative stress. *The Journal of biological chemistry.* 2007; 282:25981–25985. [PubMed: 17611193]
 11. Doucette PA, Whitson LJ, Cao X, Schirf V, Demeler B, Valentine JS, Hansen JC, Hart PJ. Dissociation of human copper-zinc superoxide dismutase dimers using chaotrope and reductant. Insights into the molecular basis for dimer stability. *J Biol Chem.* 2004; 279:54558–54566. [PubMed: 15485869]
 12. Hayward LJ, Rodriguez JA, Kim JW, Tiwari A, Goto JJ, Cabelli DE, Valentine JS, Brown RH Jr. Decreased metallation and activity in subsets of mutant superoxide dismutases associated with familial amyotrophic lateral sclerosis. *J Biol Chem.* 2002; 277:15923–15931. [PubMed: 11854284]
 13. Auclair JR, Boggio KJ, Petsko GA, Ringe D, Agar JN. Strategies for stabilizing superoxide dismutase (SOD1), the protein destabilized in the most common form of familial amyotrophic lateral sclerosis. *P Natl Acad Sci USA.* 2010; 107:21394–21399.
 14. Otwinowski Z, Minor W. Processing of X-ray diffraction data collected in oscillation mode. *Method Enzymol.* 1997; 276:307–326.
 15. Padilla JE, Yeates TO. A statistic for local intensity differences: robustness to anisotropy and pseudo-centering and utility for detecting twinning. *Acta Crystallogr D Biol Crystallogr.* 2003; 59:1124–1130. [PubMed: 12832754]
 16. Adams PD, Grosse-Kunstleve RW, Hung LW, Ioerger TR, McCoy AJ, Moriarty NW, Read RJ, Sacchettini JC, Sauter NK, Terwilliger TC. PHENIX: building new software for automated crystallographic structure determination. *Acta Crystallogr D.* 2002; 58:1948–1954. [PubMed: 12393927]
 17. Deng HX, Hentati A, Tainer JA, Iqbal Z, Cayabyab A, Hung WY, Getzoff ED, Hu P, Herzfeldt B, Roos RP, et al. Amyotrophic lateral sclerosis and structural defects in Cu,Zn superoxide dismutase. *Science.* 1993; 261:1047–1051. [PubMed: 8351519]
 18. Strong M, Sawaya MR, Wang SS, Phillips M, Cascio D, Eisenberg D. Toward the structural genomics of complexes: Crystal structure of a PE/PPE protein complex from *Mycobacterium tuberculosis*. *P Natl Acad Sci USA.* 2006; 103:8060–8065.
 19. Emsley P, Cowtan K. Coot: model-building tools for molecular graphics. *Acta Crystallogr D.* 2004; 60:2126–2132. [PubMed: 15572765]
 20. Vedadi M, Niesen FH, Allali-Hassani A, Fedorov OY, Finerty PJ Jr, Wasney GA, Yeung R, Arrowsmith C, Ball LJ, Berglund H, Hui R, Marsden BD, Nordlund P, Sundstrom M, Weigelt J, Edwards AM. Chemical screening methods to identify ligands that promote protein stability, protein crystallization, and structure determination. *Proc Natl Acad Sci U S A.* 2006; 103:15835–15840. [PubMed: 17035505]
 21. Elam JS, Taylor AB, Strange R, Antonyuk S, Doucette PA, Rodriguez JA, Hasnain SS, Hayward LJ, Valentine JS, Yeates TO, Hart PJ. Amyloid-like filaments and water-filled nanotubes formed by SOD1 mutant proteins linked to familial ALS. *Nat Struct Biol.* 2003; 10:461–467. [PubMed: 12754496]
 22. Taylor DM, Gibbs BF, Kabashi E, Minotti S, Durham HD, Agar JN. Tryptophan 32 potentiates aggregation and cytotoxicity of a copper/zinc superoxide dismutase mutant associated with familial amyotrophic lateral sclerosis. *J Biol Chem.* 2007; 282:16329–16335. [PubMed: 17389599]
 23. Fujiwara N, Nakano M, Kato S, Yoshihara D, Ookawara T, Eguchi H, Taniguchi N, Suzuki K. Oxidative modification to cysteine sulfonic acid of Cys111 in human copper-zinc superoxide dismutase. *J Biol Chem.* 2007; 282:35933–35944. [PubMed: 17913710]
 24. Ihara K, Fujiwara N, Yamaguchi Y, Torigoe H, Wakatsuki S, Taniguchi N, Suzuki K. Structural switching of Cu,Zn-superoxide dismutases at loop VI: Insights from the crystal structure of beta-mercaptoethanol modified enzyme. *Biosci Rep.* 2012
 25. Davies KJ, Goldberg AL. Proteins damaged by oxygen radicals are rapidly degraded in extracts of red blood cells. *The Journal of biological chemistry.* 1987; 262:8227–8234. [PubMed: 3597373]

26. Davies KJ, Goldberg AL. Oxygen radicals stimulate intracellular proteolysis and lipid peroxidation by independent mechanisms in erythrocytes. *The Journal of biological chemistry*. 1987; 262:8220–8226. [PubMed: 3597372]
27. Bredezen DE, Ellerby LM, Hart PJ, Wiedau-Pazos M, Valentine JS. Do posttranslational modifications of CuZnSOD lead to sporadic amyotrophic lateral sclerosis? *Ann Neurol*. 1997; 42:135–137. [PubMed: 9266721]
28. Kabashi E, Valdmanis PN, Dion P, Rouleau GA. Oxidized/misfolded superoxide dismutase-1: the cause of all amyotrophic lateral sclerosis? *Ann Neurol*. 2007; 62:553–559. [PubMed: 18074357]
29. Rakhit R, Crow JP, Lepock JR, Kondejewski LH, Cashman NR, Chakrabarty A. Monomeric Cu,Zn-superoxide dismutase is a common misfolding intermediate in the oxidation models of sporadic and familial amyotrophic lateral sclerosis. *J Biol Chem*. 2004; 279:15499–15504. [PubMed: 14734542]
30. Rakhit R, Cunningham P, Furtos-Matei A, Dahan S, Qi XF, Crow JP, Cashman NR, Kondejewski LH, Chakrabarty A. Oxidation-induced misfolding and aggregation of superoxide dismutase and its implications for amyotrophic lateral sclerosis. *J Biol Chem*. 2002; 277:47551–47556. [PubMed: 12356748]
31. Shibata N, Hirano A, Kobayashi M, Sasaki S, Kato T, Matsumoto S, Shiozawa Z, Komori T, Ikemoto A, Umahara T, et al. Cu/Zn superoxide dismutase-like immunoreactivity in Lewy body-like inclusions of sporadic amyotrophic lateral sclerosis. *Neurosci Lett*. 1994; 179:149–152. [PubMed: 7845611]
32. Choi J, Rees HD, Weintraub ST, Levey AI, Chin LS, Li L. Oxidative modifications and aggregation of Cu,Zn-superoxide dismutase associated with Alzheimer and Parkinson diseases. *J Biol Chem*. 2005; 280:11648–11655. [PubMed: 15659387]
33. Molnar KS, Karabacak NM, Johnson JL, Wang Q, Tiwari A, Hayward LJ, Coales SJ, Hamuro Y, Agar JN. A common property of amyotrophic lateral sclerosis-associated variants: destabilization of the copper/zinc superoxide dismutase electrostatic loop. *J Biol Chem*. 2009; 284:30965–30973. [PubMed: 19635794]
34. Hornberg A, Logan DT, Marklund SL, Oliveberg M. The coupling between disulphide status, metallation and dimer interface strength in Cu/Zn superoxide dismutase. *J Mol Biol*. 2007; 365:333–342. [PubMed: 17070542]
35. Rakhit R, Robertson J, Vande Velde C, Horne P, Ruth DM, Griffin J, Cleveland DW, Cashman NR, Chakrabarty A. An immunological epitope selective for pathological monomer-misfolded SOD1 in ALS. *Nat Med*. 2007; 13:754–759. [PubMed: 17486090]

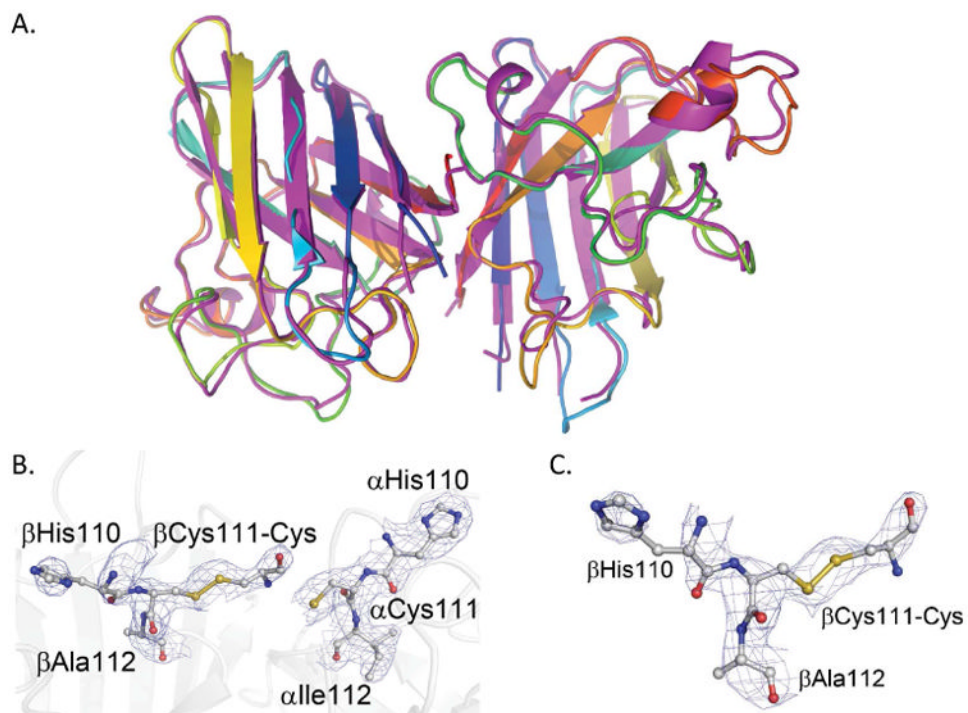


Figure 1. Cysteinylation of Cys₁₁₁ in SOD1

(A.) Structure of cysteinylated SOD1 dimer (magenta) superimposed with wild type SOD1 (PDB ID: 1SPD¹⁷). The global structure is conserved in the cysteinylated SOD1. (B and C.) Cysteinylation is observed only on chain β . Zoom in of the cysteinylated Cys₁₁₁ with electron density contoured at 1/sigma.

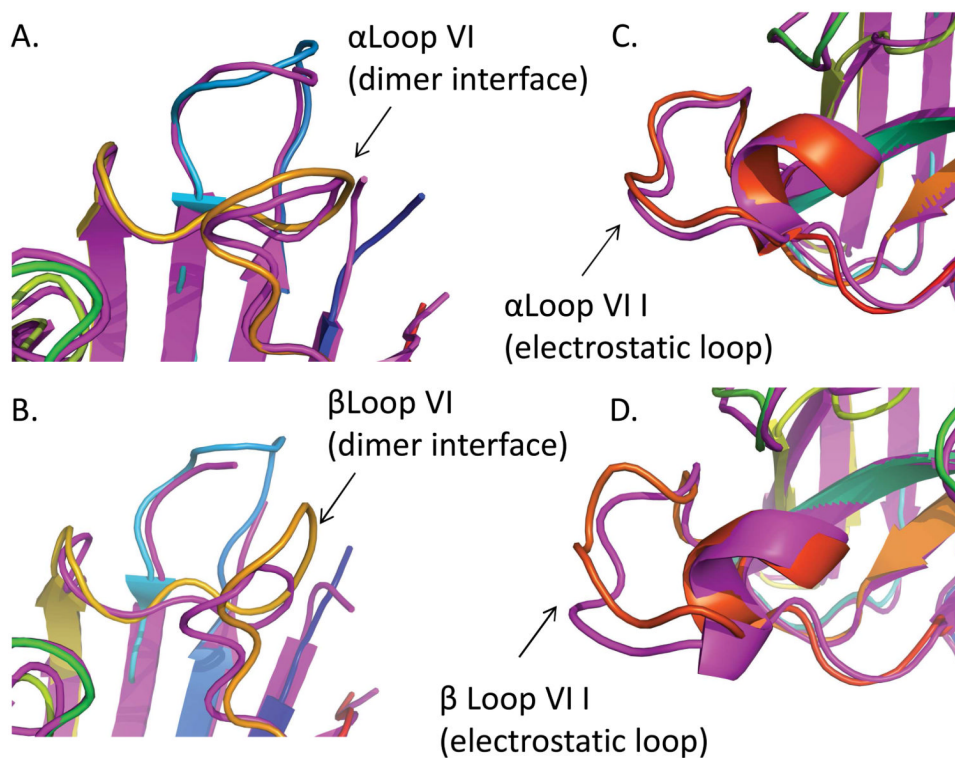


Figure 2. Cysteinylation caused local structural changes in SOD1

Structure of cysteinylated SOD1 dimer (magenta) superimposed with wild type SOD1 (PDB ID: 1SPD¹⁷). Cys₁₁₁-cys loop VI (magenta) overlaid with 1SPD¹⁷ showing small changes in the region where no cysteinylation is observed (A.) and large, local, structural changes at the site of modification on chain β (B.). The electrostatic loop of the unmodified monomer is similar to SOD1 (PDB ID: 1SPD¹⁷) (C.), whereas the electrostatic loop of the modified monomer undergoes a conformational change (D.).

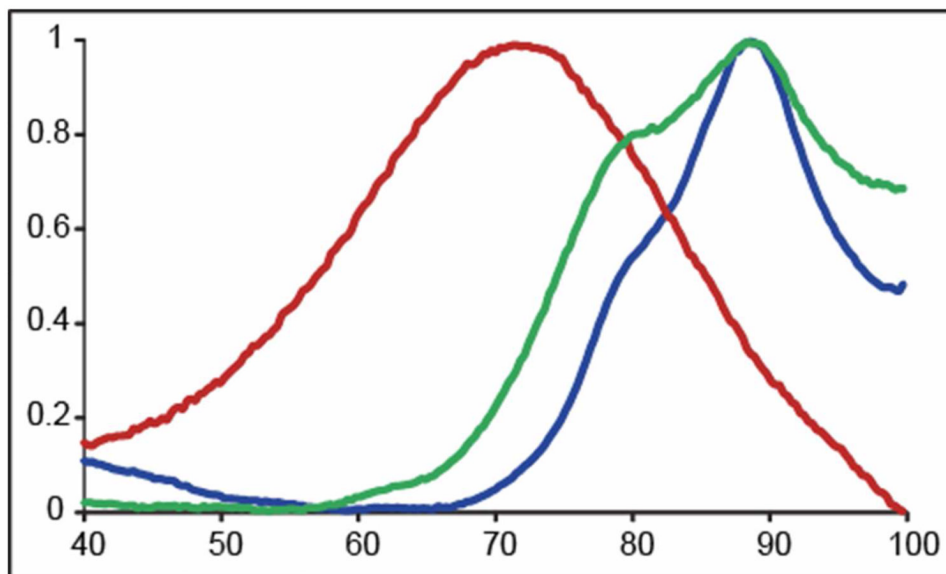


Figure 3. Oxidation and Cysteinylation destabilized SOD1

Differential scanning fluorimetry was used to measure the melting temperature of SOD1, peroxide oxidized SOD1, and SOD-1 cys. Melting temperature of SOD1 (blue), peroxide oxidized SOD1 (red), and cysteinylated SOD1 (green). Oxidation destabilized SOD1 by approximately 23 °C whereas cysteinylation destabilized SOD1 by approximately 5 °C. Folding-unfolding transitions (thermal denaturation curves) were measured in triplicate.

Table 1

Crystallographic data and refinement statistics.

Data collection statistics	SOD-cys
Beam line	APS, GM/CA-CAT, ID-B
Wavelength	0.95 Å
Space group	$P6_3$
Cell constants	$a = 113.1 \text{ \AA}$ $b = 113.1 \text{ \AA}$ $c = 70.6 \text{ \AA}$ $\alpha = \beta = 90^\circ$ $\gamma = 120^\circ$
Total reflections	16978
Unique reflections	15290
Resolution limit (Å)	2.48 (2.48-2.57) *
Completeness (%)	94.8 (100.0)
Redundancy	10.9 (10.7)
$I/\sigma I$	25.6 (4.8)
R_{merge} (%)	0.083 (0.56)
Refinement statistics	SOD-cys
Resolution range (Å)	2.48-27.15
R_{free} test set size	1688
R_{work} (%)	27.6
R_{free} (%)	33.5
No. Atoms	
Total	2221
Protein	2193
Water	24
Copper	2
Zinc	2
B-factors	
Overall	52.13
R.m.s. deviations	
Bond lengths (Å)	0.009
Bond angles (°)	1.3

* parenthesis are for statistics in the highest resolution shell.